2016

High-Resolution Ground-Penetrating Radar Profiles of Perennial Lake Ice in the McMurdo Dry Valleys, Antarctica: Horizon Attributes, Unconformities, and Subbottom

Hilary A. Dugan
University of Wisconsin - Madison

Steven A. Arcone
U.S. Army Engineer Research and Development Center

Maciej K. Obryk
Portland State University, mobryk@pdx.edu

Peter T. Doran
Louisiana State University

Citation Details

Dugan, H. A., Arcone, S. A., Obryk, M. K., & Doran, P. T. (2015). High-resolution ground-penetrating radar profiles of perennial lake ice in the McMurdo Dry Valleys, Antarctica: Horizon attributes, unconformities, and subbottom penetration. Geophysics, 81(1), WA13-WA20.

GEOPHYSICS, VOL. 81, NO. 1 (JANUARY-FEBRUARY 2016); P. WA13–WA20, 7 FIGS., 1 TABLE.
10.1190/GEO2015-0159.1

High-resolution ground-penetrating radar profiles of perennial lake ice in the McMurdo Dry Valleys, Antarctica: Horizon attributes, unconformities, and subbottom penetration

Hilary A. Dugan[1], Steven A. Arcone[2], Maciej K. Obryk[3], and Peter T. Doran[4]

ABSTRACT

Ground-penetrating radar (GPR) is not commonly used to study lake ice, and in general, the ground-based use of radar frequencies greater than 500 MHz in cryosphere geophysics is rare, due to a general interest in deeper stratigraphy and the difficulty of extensive profiling over rough snow surfaces. Our goal was to find further information on the origin of the deposition and formation of intra-ice layers, bottom topography, and subbottom deposits using GPR with pulses centered near 850 MHz on two permanently ice-covered lakes in the McMurdo Dry Valleys, Antarctica. The profiles were obtained using a one-person sled operation over Lake Bonney, which is typical of lakes in the region, having an ice thickness that ranges between 3 and 5 m, and Lake Vida, where the maximum ice depth is at least 27 m. Lake Bonney exhibits a semicontinuous sediment horizon at approximately a 2-m depth and several minor horizons. In contrast, Lake Vida contains unconformably eroded and folded continuous reflection horizons, packages of minor horizons between major horizons, evidence of incised fluvial deposition along the bottom, and subbottom penetration of at least 4.5 m in some areas. Where the ice thickness is less than 20 m, the lake is frozen to the bottom. Most horizon waveform phase attributes indicate relatively lower permittivity than in the surrounding matrix. Consequently, we interpreted these strata to be caused by layers of pure ice embedded within a salty and dirty ice matrix, which were formed during minor flooding. These findings supported previous conclusions that Lake Vida ice formed from surface runoff in combination with periods of ablation.

INTRODUCTION

Perennially ice-covered lakes are unusual on the earth, being found mostly in the Antarctic with a few examples in the Arctic (Doran et al., 2004). In comparison with the well-known formation of temperate and polar seasonal lake ice, and multiyear sea ice (Thomas and Dieckmann, 2010), perennial lake ice is relatively understudied. The most well-researched perennial lake ice exists on the closed-basin lakes of the McMurdo Dry Valleys (MDV) of Antarctica, in part because it is a viable habitat for microbial communities (Fritsen and Priscu, 1998; Priscu et al., 1998). Physical studies have evaluated ablation rates (Clow et al., 1988; Dugan et al., 2013), sediment melt migration rate into the ice covers (Jepsen et al., 2010), internal ice stratigraphy (Adams et al., 1998), an energy balance approach to predicting ice thickness (McKay et al., 1985), and historic hydrologic changes (Dugan et al., 2015b). However, many of these studies draw conclusions from observations at one to a few sites, typically in the center of the lake, which are then assumed to apply across the lake. Little is known about the spatial characteristics of perennial lake ice and its genesis.

Here, we discuss several high-resolution ground-penetrating radar (GPR) profiles obtained across two MDV lakes, Lake Bonney and Lake Vida, which reveal details about the stratigraphic genesis of perennial lake ice. Our objective was to record GPR profiles across the entire lake and with enough time range to record any subbottom penetration. We used 850-MHz (bandwidth-centered)

Manuscript received by the Editor 7 March 2015; revised manuscript received 1 May 2015; published online 28 August 2015.
[1]University of Wisconsin-Madison, Center for Limnology, Madison, Wisconsin and Cary Institute of Ecosystem Studies, Millbrook, New York, USA. E-mail: hilarydugan@gmail.com.
[2]U.S. Army Engineer Research and Development Center — Cold Regions Research and Engineering Laboratory, Hanover, New Hampshire, USA. E-mail: steven.a.arcone@erdc.dren.mil.
[3]Portland State University, Department of Geology, Portland, Oregon, USA. E-mail: mobryk@pdx.edu.
[4]Louisiana State University, Department of Geology and Geophysics, Baton Rouge, Louisiana, USA. E-mail: pdoran@lsu.edu.

pulses in expectation of recording detailed stratigraphy at a 15-cm horizon resolution, and possibly penetrating ice-rich sediments. Until our work, the use of such high-frequency surface-based GPR in Antarctica had only been used to investigate the firn of polar ice sheets (Kanagaratnam et al., 2001, 2004; Langley et al., 2007, 2009). In the MDV, GPR has been applied in glacial (Arcone and Kreutz, 2009; Shean and Marchant, 2010) and permafrost (Arcone et al., 2002; Bristow et al., 2010) settings, but at frequencies of less than 500 MHz.

This investigation further develops recent findings from ice cores and from lower resolution 400-MHz GPR on Lake Vida that showed that the entire known ice cover formed from surface runoff, that the sediment layers in the ice represent accumulation of surface deposits, and that the ice cover has been subjected to ablation (Dugan et al., 2015a, 2015b). However, greater resolution was needed to determine any structure to the horizons. Here, we examine GPR profiles in more detail to reveal processes that contributed to the deposition, ablation, and horizon formation. We also compare results from Lake Bonney with those obtained by a large-scale deployment of an autonomous underwater vehicle used to map the ice thickness and sediment distribution in part of the lake (Obryk et al., 2014).

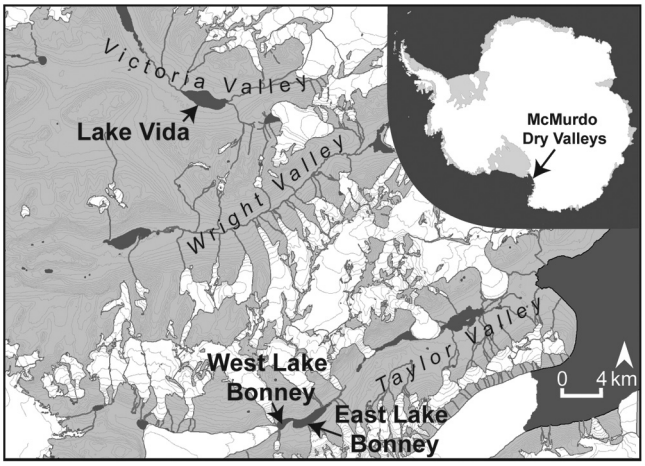

Figure 1. Location of Lake Vida and Lake Bonney in the MDV, Antarctica.

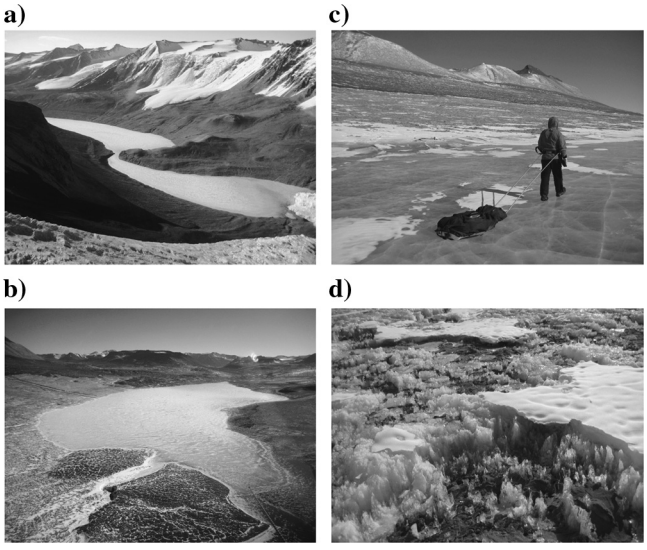

Figure 2. (a) Lake Bonney, Taylor Valley, viewed from the northwest. WLB is in the foreground, and ELB is in the background. Taylor Glacier can be seen abutting WLB on the far right of the photo. (b) Lake Vida, Victoria Valley, viewed from the east. (c) GPR survey on Lake Vida. (d) Ablation surface on the eastern edge of Lake Vida.

METHODS

Location

Lake Bonney, in Taylor Valley (77.72 S, 162.30 E), and Lake Vida, in Victoria Valley (77.39 S, 161.93 E), Antarctica (Figure 1) are closed basin and permanently ice covered (Figure 2a and 2b). Lake Bonney is a proglacial lake that abuts Taylor Glacier in Taylor Valley. The lake is 4.3 km^2 in area, and it is divided into two lobes, identified as the east lobe of Lake Bonney (ELB) and the west lobe of Lake Bonney (WLB). The Long Term Ecological Research Program operating in Taylor Valley has measured ice thickness at a central location on ELB and WLB from 1996 to present. Measurements taken during the austral spring (October to December) have ranged from 3.31 (2008) to 5.00 m (2004) on ELB and 3.41 (2009) to 4.54 (2001) on WLB (Priscu, 2015).

Lake Vida is 6.8 km^2 in area, and it is unique in that it has the thickest ice cover of any known surface lake on earth (Dugan et al., 2015b). Ice coring on Lake Vida has reached 27 m, and from an airborne electromagnetic study, it is hypothesized that the ice could be as thick as 45 m (Dugan et al., 2015a). In 2011, the ice cover on both lakes was relatively smooth (Figure 2c), which insured almost-continuous contact between the GPR sled and the lake ice. Only on the edges of both lakes did significant ablation surfaces obscure penetration (Figure 2d).

Ground-penetrating radar

GPR surveys were conducted with a Geophysical Survey Instruments, Inc. (GSSI), SIR-3000, 16 bit, 1-channel acquisition unit and a model 3101 900-MHz antenna on 16–18 November 2011. The actual bandwidth-centered pulse frequency was 850 MHz, providing a 30-cm-long in situ pulse (examples given below) with 15-cm horizon resolution in the ice assuming a relative dielectric permittivity of $\varepsilon = 3.15$. On Lake Vida, we recorded at a time range of 400 ns and we used 2048 samples per trace; on Lake Bonney, we needed only 100 ns. Assuming $\varepsilon = 3.15$, a 400-ns traveltime provides a range of 33.8 m, and 100 ns provides 8.5 m. We processed with a two-pole band-pass filter (400–1300 MHz), applied background removal, and then automatic range gain to approximately equalize gain across each trace. The 2D migration of the data showed no improvement in the image, and it is not applied in our results. However, we did check our radio-wave speeds using software (RADAN7; GSSI)-supplied hyperbola models, which showed that our ε value was correct within 4% error on Lake Vida; the radio-wave speed in the ice is discussed later.

Typically, in early December on Lake Bonney, the ice cover becomes isothermal and porous to lake water as the surface air temper-

atures increase. At the time of the survey, drilling revealed that the ice cover on Lake Bonney had not reached this stage, which created favorable conditions for radar acquisition. The GPR system was transported on a fiberglass sled that was pulled across the ice surface (Figure 2c). On Lake Vida, one individual with a handheld global positioning system (GPS) pulled the sled at speeds averaging 4.5 km h^{-1} to collect 14 km of data. On Lake Bonney, the sled was attached behind an all-terrain vehicle that was equipped with a differential GPS and maintained speeds averaging 5–5.5 km h^{-1}. We collected 11 km of transects on ELB and 7 km of transects on WLB.

Manual ice thickness measurements near the center of each lake ranged from 3.82 to 3.87 m on ELB from 14–15 November 2011 and 3.68–3.74 m on WLB from 15–22 November 2011 (Priscu, 2015). An ε value and corresponding depth scales were calibrated from transects that coincided with these observed ice thickness measurements in the center of the two lobes. For Lake Bonney, $\varepsilon = 3.2$.

Data from Lake Bonney were analyzed in R statistical software (R Core Team, 2015). The mean ice surface depth of each survey was adjusted to zero, and ice depths were calculated based on the traveltime to the bottom reflection of the ice and calculated ε. A thresholding routine was used to automate the picking of the ice depth and sediment layers where possible. For each transect, a rolling median filter was applied to smooth ice thickness data. A bicubic spline interpolation routine for irregularly spaced data was then applied to map ice thickness in 20 m^2 bins across WLB.

RESULTS

Lake Bonney

In 2011, the ice cover of Lake Bonney was relatively smooth, and ablation surfaces only impeded GPR efficacy on the northern edge of WLB. Overall, GPR was easily able to penetrate the ice cover on both lobes. Distinct horizons approximately 3.5–4 m below the surface are present in all transects (Figure 3). The ice cover thickness was fairly uniform across both lobes, excluding the lake edges, where the ice began to thin. On WLB, the mean thickness for each transect ranged from 3.44 to 3.84 m, and on WLB, from 3.62 to 3.99 m, all with low standard deviations (Table 1). In general, the lake ice thinned from north to south (Figure 4). In many cases, a second horizon was detectable approximately 1.5–3 m below the ice surface, which also had a phase structure denoting high to low permittivity. For example, on ELB in transect #24, this secondary horizon was always slightly more than 2 m, whereas on WLB in transect #17, it was consistently less than 2 m. Near the edges of the lake, where the ice cover begins to thin, this internal layer disappears (Figure 3a).

Automating the picking of the bottom of the ice cover appears to be an effective routine to simplify mapping of ice cover thickness (Figure 4). Only at select points does this routine seem to fail, but it is unclear whether this is a result of the ice thickness estimate or spline interpolation routine. Accurately automating the picking of the internal layer was difficult, and results appear to pick too deeply, and overestimate the location in many instances (Figure 3c). Therefore, mapping the depth to the internal horizon was not attempted.

Lake Vida

Lower resolution (400 MHz; 30-cm vertical horizon resolution) GPR has been used on Lake Vida to assess the thickness of the ice and general stratigraphy (Dugan et al., 2015b). Here, we focus on the more detailed stratigraphy and the bed-ice contact. Transects across the middle of the lake show distinct primary layers with strong horizontal continuity across the lake (Figure 5a). The profile shows several stratigraphic regimes, including one that is folded, one that is eroded and slightly buckled with distinct rhythmic depositional horizons, and two without rhythmic deposition. There is a prominent angular unconformity between the folded and rhythmic regimes, the ends of which have rough interfaces (Figure 5a). From approximately 8- to 14-m depth, multiple horizons appear between the brighter horizons (Figure 5b). An isolated reflected waveform shows the same half-cycle phase polarity sequence (negative-positive-negative; aka – + –), which indicates that the horizons represent a relatively low-permittivity layer within the ice matrix (Arcone et al., 2002). This pulse attribute is peculiar to the antennas

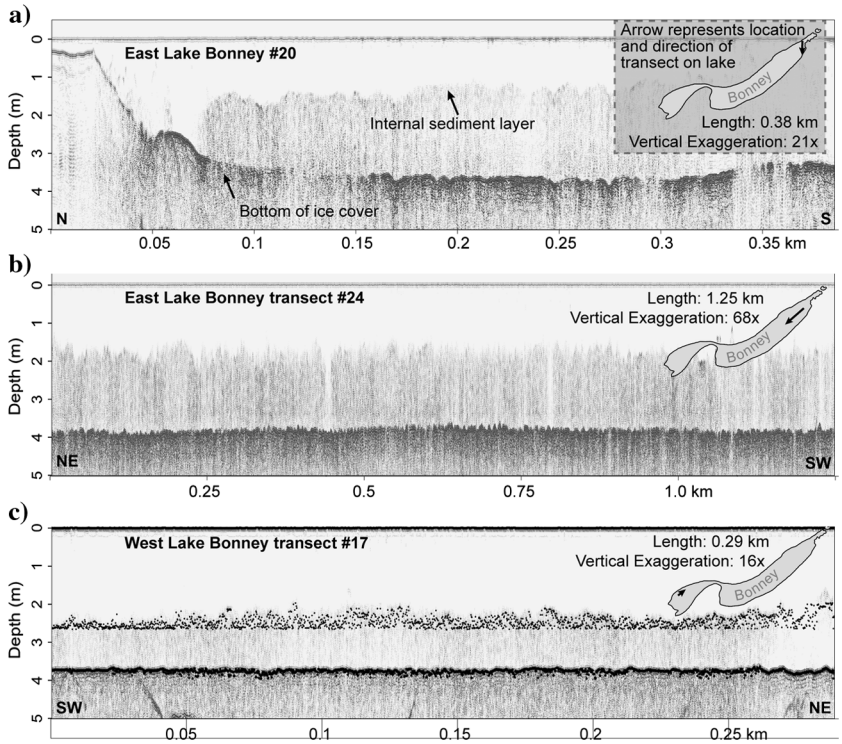

Figure 3. (a) Transect at the eastern edge of ELB from north to south. At the edge of the lake (left side), the ice cover is very thin, and no internal sediment layer or change in ice morphology with depth is detected. By 50 m into the profile, the ice cover has reached almost 4 m in thickness and the internal horizon is present. (b) A 1.25 km transect of ELB showing relatively consistent ice thickness. (c) Automated picking of the bottom of the ice cover (lower black dots) and internal sediment layer (upper black dots) in a WLB transect.

of this manufacturer (other commercial systems may radiate a different phase polarity sequence). Along the shore at left is evidence of at least 4.5 m of subbottom penetration, calculated from a realistic $\varepsilon = 5.5$ for ice-rich sediments (Arcone et al., 2002). At this depth, the lake bed is expected to be frozen (Dugan et al., 2015b). The apparent lake bottom horizon also has a – + – half-cycle sequence, indicating a lower value of ε than the surrounding matrix. At the edges of the lake, near the mouth of two major rivers, ice folding, rhythmic horizons, and subbottom penetration are all evident (Figure 6).

Figure 6 shows three examples from the near shore environment. Figure 6a shows a short section with a horizon of sufficiently strong reflectivity to cause multiple reflections. This is followed by complexly folded and eroded strata, and irregular 20- to 50-cm-high hummocks on the lake bed from 8- to 10-m depth. Figure 6b shows a 5 m tall hump in the subbottom stratigraphy with associated upturned strata on both sides. Figure 6c shows an apparent slump defined by a clear bottom horizon below the near shore shelf. The heavy arrow in this figure indicates subbottom penetration of possibly more than 5 m. Just to its right is a short reflective section that has two multiple reflections that follow.

Table 1. Mean ice thicknesses and standard deviations across ELB and WLB, generated from an automated picking routing with $\varepsilon = 3.2$.

Transect	Length (m)	Mean (m)	St. dev. (m)
West Lake Bonney			
10	303	3.81	0.04
11	602	3.63	0.07
13	311	3.47	0.07
14	190	3.44	0.04
15	466	3.64	0.08
17	288	3.76	0.02
18	308	3.78	0.03
21	264	3.69	0.03
23	246	3.56	0.10
24	411	3.79	0.05
25	181	3.66	0.09
26	365	3.73	0.06
27	409	3.77	0.08
28	287	3.84	0.05
29	190	3.77	0.02
30	119	3.84	0.02
33	1289	3.66	0.06
35	569	3.64	0.09
East Lake Bonney			
6	839	3.84	0.07
7	814	3.86	0.05
9	924	3.87	0.04
11	548	3.99	0.03
13	402	3.95	0.05
16	941	3.80	0.09
18	720	3.84	0.09
20	385	3.62	0.11
22	216	3.68	0.14
24	1246	3.83	0.05
103	321	3.84	0.05
106	2460	3.77	0.08

DISCUSSION AND INTERPRETATION

Lake Bonney

There are two major outcomes from our GPR surveys of ELB and WLB. The first is that the ice cover thickness is fairly uniform, apart from the first-year ice on the lake edges. Overall, calculated ice thickness on ELB is slightly thicker than WLB, which agrees with manual measurements. Our results also compare well with those returned from an underwater survey acquired using a large autonomous underwater vehicle (Obryk et al., 2014). In that study, the ice on WLB was found to thicken by 70 cm from the southern to northern shoreline, in comparison with the approximately 50 cm we estimate. Obryk et al. (2014) report the ice thickness in its water equivalent, whereas we report uncorrected ice thickness. In general, our spatial estimates of ice thickness agree with those found by Obryk et al. (2014), and they support our simple methodology. Additionally, we validate the assumption by Obryk et al. (2014) of consistent ice thickness patterns from year to year.

The second finding is an internal reflector present in all transects that either corresponds to an area of high sediment density formed from the downward movement of surface sediment into the ice cover or denotes a transition in ice morphology. Sediment accumulates within the ice cover as dark sediment deposited on the ice surface absorbs solar radiation and preferentially melts downward within the frozen ice cover. This process is well described in the literature (Nedell et al., 1987; Squyres et al., 1991; Priscu et al.,

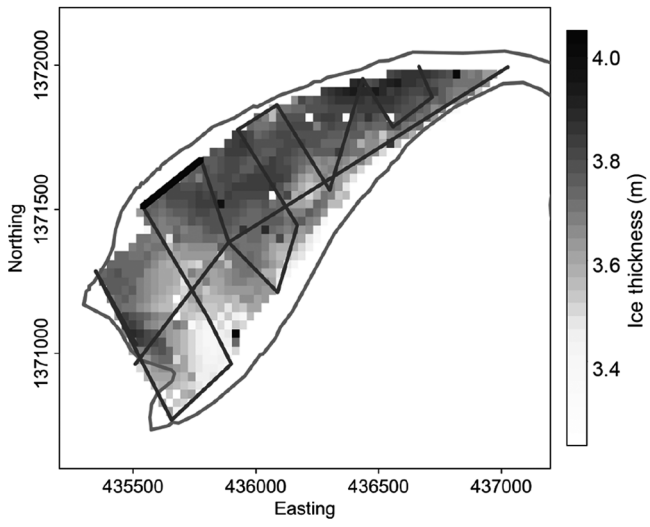

Figure 4. (a) Spatial interpolation of ice thickness on Lake Bonney using a bicubic spline routine. The gray lines denote GPR transects and the edge of the lake. Transect #17 (show in Figure 3c) is highlighted in black.

1998; Jepsen et al., 2010), and it has been shown to be able to penetrate to approximately 2-m depth based on an energy balance model. The sediment usually clumps within discrete packets, rather than as a continuous layer (Adams et al., 1998; Obryk et al., 2014), and it can be envisioned as a heterogeneous band within the ice cover. Ice morphology below this sediment band changes to a clear ice with vertical chains of air bubbles, presumably an indication of winter ice growth (McKay et al., 1994; Adams et al., 1998). We find the internal layer on both lakes fluctuates approximately 2-m depth, which is consistent with observations from drillhole measurements and literature. This is the first time it has been spatially characterized. In all transects near the edges of Lake Bonney, the internal horizon is not present. This is attributable to the fact that all ice at the edge of the lake is first-year ice that melts during the austral summer. Therefore, the internal horizon could be used to map the extent of multiyear ice on the lake.

Lake Vida

Cause of horizons, subbottom penetration, and the matrix ε

Nearly every horizon exhibits the same – + – phase structure, indicating a relatively low permittivity layer. Even the apparent lake bottom horizon has this structure. This can only be caused either by a layer of low-density ice, such as hoar or eroded ice, or by the ice matrix ε being actually slightly higher, so that these horizons represent layers of pure ice. As mentioned above, measurements of ice thickness on Lake Bonney provide $\varepsilon = 3.2$, and the ice on Lake Vida may contain more salts because they cannot be rejected into the water column due to new ice-forming layers on top of old ice (Dugan et al., 2015a). Values of $\varepsilon > 3.2$ at very cold temperatures have been measured in the laboratory on artificially grown sea ice (Arcone et al., 1986). An ε as high as 3.4 would shrink the depth scale of our figures by only 4%. Below the bottom horizon, the underlying ice is sediment rich, which elevates the ε of the subbottom and would also help to cause this phase structure, given that the ice just above the bottom layer may be slightly salty.

Subbottom penetration of Lake Vida was possible because the ice is grounded to the bed in the upper 20 m, like a cold-based glacier (Dugan et al., 2015a). This penetration of at least 4 m could only be achieved in frozen, ice-rich sediments, especially at 850 MHz. The sediment could contain coarse gravel and still avoid imposing scattering losses, so long as the particle sizes were less than the in situ wavelength (Liu et al., 2013). The finding by Murray et al. (2012) and Dugan et al. (2015a) that the brine reservoir lies several meters below the lake ice is consistent with this depth of penetration. Our ability to effectively image shallow lake bed features, is similar to investigations using GPR on cold, temperate freshwater lakes (Fuchs et al., 2004; Parker, 2010).

Primary and multiple horizons

We interpret all of the horizons to comprise primary reflections from layers that are thinner than the pulse wavelength of 30 cm. In this case, there are no multiple intralayer reflections. As a thin layer thickens, an extra oscillation of equal amplitude will first appear, and then finally a multiple separates. For example, at 850 MHz and $\varepsilon = 3.15$ for a fresh water layer, the in situ wavelength is approximately 20 cm (2/3 pulse wavelength). If the surrounding matrix has $\varepsilon = 3.3$, then a 9 cm layer is required to produce one extra half-cycle, which is as strong as the previous half-cycle (Figure 7). Therefore, for layers <8 cm in thickness, there are no multiples. If the layer was 30-cm thick, then there would be two distinct and equally strong pulses, but with the second having the phase reversed. In Lake Vida, there is no indication of this, only pure wavelets with only three half-cycles (Figure 5b). Consequently, the lower amplitude oscillations between these distinct pulses are also likely primary reflections, but they are too close to resolve, and so they appear as if they are multiples. At a 400-MHz resolution, some primary reflections overlap to give the appearance of intralayer multiples (Figure 5c).

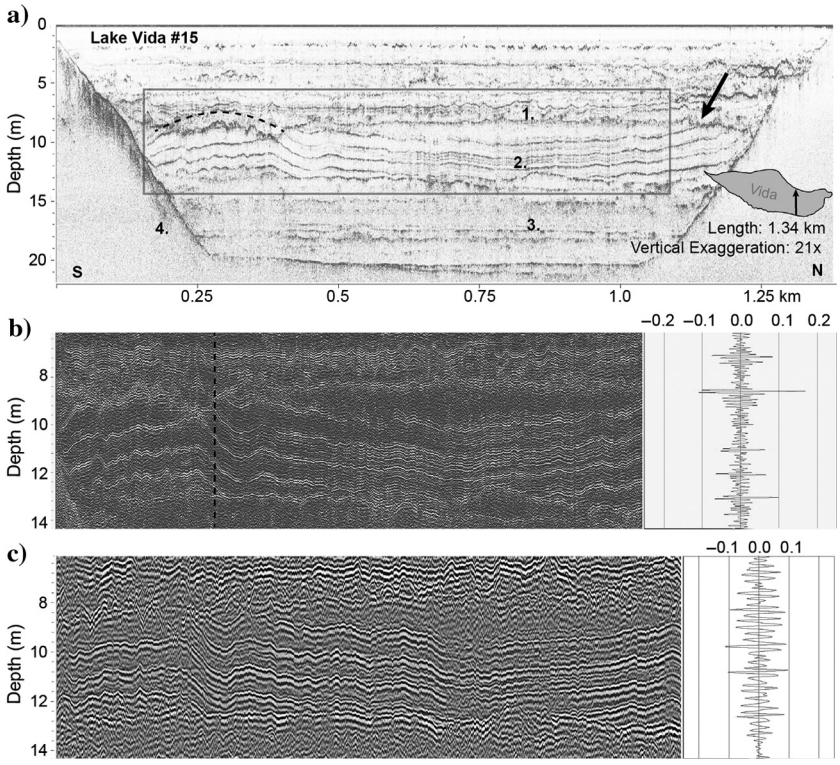

Figure 5. (a) Complete profile of 850 MHz transect #15 south to north across Lake Vida. Outline of lake and arrow denotes location of transect. Labeled stages of deposition include (1) a folded regime, (2) an eroded and buckled regime with distinct rhythmic depositional horizons, (3) regimes without rhythmic deposition, and (4) subbottom penetration. Angular unconformity is noted with black arrow. The more obvious unconformities are shown with a dashed line as a hypothetical reconstruction of an eroded layer. (b) Detail of a section bordered by box in panel (a) and waveform of trace (dashed line) at 415.7 m distance. Secondary horizons appear between the primary horizons. The reflected waveforms seen at right all show the same phase polarity sequence (– + –), which indicates a relatively lower permittivity thin layer within the ice matrix. (c) Detail of a section from a transect recorded in 2010 at 400 MHz. At a lower resolution, reflected horizons are not as distinct, overlap others, and provide intralayer multiples.

Unconformities

During our survey, we find major unconformities and strong erosion of the surface near the shores (Figures 5 and 6). The superimposed dashed line is a hypothetical reconstruction of the original ice (Figure 5). Consequently, it appears that the erosion took place as the ice buckled, and the buckling was most significant near the shores.

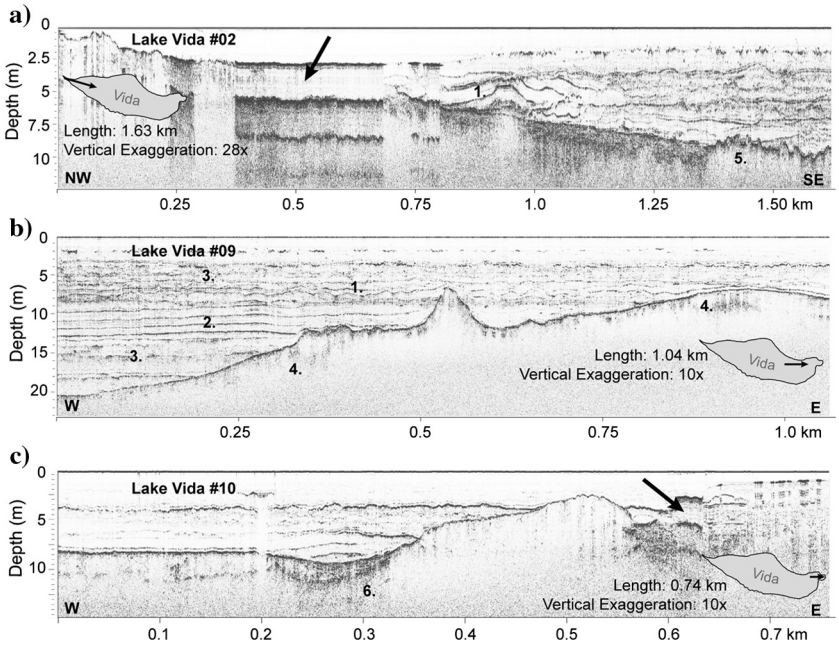

Figure 6. GPR transects on the edges of Lake Vida near the mouth of inflowing rivers. All number labels refer to same features seen in Figure 5. (a) Near the shore, there are multiple folded horizons and (5) irregular bed features. Surface ablation features and/or melt pools may have generated multiple reflections (black arrow). (b) Transect #9 showing what appears to be either an intrusion or bottom deposit. (c) Transect #10 showing (6) possible slump deposits at the foot of a bottom mound.

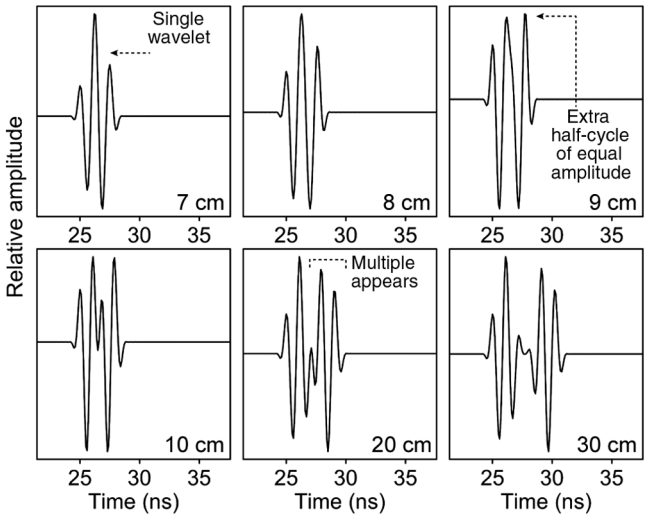

Figure 7. Theoretical 850 MHz GPR pulse reflections from a thin layer of fresher ice with $\varepsilon = 3.15$, embedded in less fresh ice with $\varepsilon = 3.3$. The layer is 2 m deep with thicknesses labeled. By 9 cm, the pulse shows resonance.

Folding and buckling

Folding or possible buckling occurs both at a large scale (Figure 5, across most of the basin) and at a small scale. The small scale buckling is peculiar because it occurs only within a few meters thickness. We suggest that this ice may be extra saline and plastic, and possibly buckled independently of the ice above and below it, having moved slowly along saline planes of weakness. Most peculiar is the symmetrical hump along the bottom (Figure 6b). The strata surrounding it are upturned, as if this hump represents an upward intrusion that displaced and compressed the ice. It seems unlikely that the ice around it has undergone compression from both ends of the lake. One explanation may be that the mound is a salt intrusion or a salt-rich pingo.

Fluvial bedforms

The unusual geomorphic features on the lake bed near the edges of Lake Vida may be explained by the fact that the lake level has been rising for the past three decades (Barrett et al., 2008; Doran, 2015), and it is calculated to have risen approximately 8 m over the past century (Dugan et al., 2015b). There are three rivers that flow into Lake Vida, one at the west end that drains from Upper Victoria Glacier, and two at the east that drain from Lower Victoria Glacier and Clark Glacier. In all three cases, the mouth of the river follows an incised channel into the lake. It is likely that as the lake level has risen, ice has accreted on the top of, and therefore preserved, fluvial geomorphic features (Figure 6). Near the eastern edge of Lake Vida, a concave dip in the ice-bed contact may be a relic river channel, with infilled scour above it (Figure 6c). Apparent discontinuities, approximately 5-m below the surface at the western and eastern edges of the lake, could be fictional due to ablated surface conditions near the edge of the lake interfering with signal paths, or could represent brine/water pockets trapped in the upper ice (black arrows in Figure 6a and 6c).

CONCLUSION

Our 850-MHz profiles provide images of unusual lake features for which our explanations are provisional, but supply new hypotheses for further investigation. Localized folding and bottom intrusion are likely consequences of the saline nature of the lake ice and of the bottom sediment-rich ice, respectively. We recommend surveys with lower-frequency antennas for gathering more subbottom information to see if any such structures have subsurface origins or if they are a bottom depositional feature.

This high-frequency GPR has proved an effective geophysical tool for investigating the stratigraphy of lake ice on two contrasting polar lake systems. In this setting, it is a simple and cost effective tool that can help us to understand spatial limnological characteristics. Drawn from these investigations, the following are potential applications of GPR on multiyear lake ice:

1) *Mapping ice thickness*: Ice thickness measurements are usually recorded from ice holes augured through the ice pack. As little as one in situ measurement could be used to calibrate GPR surveys across the entire ice cover.
2) *Resolving perennial ice*: The change in ice morphology and presence of sediment in the ice cover may indicate the presence of perennial ice, as models suggest two years for sediment to migrate 2-m downward (Jepsen et al., 2010). This information would be valuable in settings that experience total ice loss only in some years (Paquette et al., 2015).
3) *Mapping internal horizons*: Sediment layers in the lake ice provide a unique habitat for microbial communities to thrive in (Priscu et al., 1998). Here, we show that the vertical displacement of sediment into an ice pack can be spatially delineated.

Future studies should correlate internal horizons resolved in GPR with total sediment concentration or the chemical composition of the ice, or the lack thereof. Sediment load in the ice cover is an important regulator of light transmission into the water column, which is essential for autotrophic primary productivity. Quantification of sediment load could be an effective means of estimating ecosystem habitability in the underlying water column.

ACKNOWLEDGMENTS

We would like to thank PHI helicopters for their dedicated and safe work. This research was funded by the United States National Science Foundation Office of Polar Programs (grant no. 1115245). Raytheon Polar Services Company (RPSC) Field Safety and Training Program under the United States Antarctic Program provided an equipment loan.

REFERENCES

Adams, E. E., J. C. Priscu, C. H. Fritsen, S. R. Smith, and S. L. Brackman, 1998, Permanent ice covers of the McMurdo Dry Valley lakes, Antarctica: Bubble formation and metamorphism, *in* J. C. Priscu, ed., Ecosystem dynamics in a polar desert: The McMurdo Dry Valleys, Antarctica: American Geophysical Union, 281–295.

Arcone, S. A., A. J. Gow, and S. McGrew, 1986, Structure and dielectric properties at 4.8 and 9.5 GHz of saline ice: Journal of Geophysical Research, **91**, 14281, doi: 10.1029/JC091iC12p14281.

Arcone, S. A., and K. Kreutz, 2009, GPR reflection profiles of Clark and Commonwealth Glaciers, Dry Valleys, Antarctica: Annals of Glaciology, **50**, 121–129, doi: 10.3189/172756409789097531.

Arcone, S. A., M. L. Prentice, and A. Delaney, 2002, Stratigraphic profiling with ground-penetrating radar in permafrost: A review of possible analogs for mars: Journal of Geophysical Research, **107**, 5108, doi: 10.1029/2002JE001906.

Barrett, J. E., R. A. Virginia, D. H. Wall, P. T. Doran, A. G. Fountain, K. A. Welch, and W. B. Lyons, 2008, Persistent effects of a discrete warming event on a polar desert ecosystem: Global Change Biology, **14**, 2249–2261, doi: 10.1111/j.1365-2486.2008.01641.x.

Bristow, C. S., P. C. Augustinus, I. C. Wallis, H. M. Jol, and E. J. Rhodes, 2010, Investigation of the age and migration of reversing dunes in Antarctica using GPR and OSL, with implications for GPR on mars: Earth and Planetary Science Letters, **289**, 30–42, doi: 10.1016/j.epsl.2009.10.026.

Clow, G. D., C. P. McKay, G. M. Simmons, and R. A. Wharton Jr., 1988, Climatological observations and predicted sublimation rates at Lake Hoare, Antarctica: Journal of Climate, **1**, 715–728, doi: 10.1175/1520-0442(1988)001<0715:COAPSR>2.0.CO;2.

Doran, P. T., 2015, McMurdo Dry Valley lake levels: Long term ecological research network, 10.6073/pasta/112812a4c1579a00b6bb6f7f26ab39fd, accessed 02 April 2015.

Doran, P. T., J. C. Priscu, W. B. Lyons, R. D. Powell, D. T. Andersen, and R. J. Poreda, 2004, Paleolimnology of extreme cold terrestrial and extraterrestrial environments, *in* R. Pienitz, M. S. V. Douglas, and J. P. Smol, eds., Long-term environmental change in Arctic and Antarctic lakes: Springer, 281–295.

Dugan, H. A., P. T. Doran, S. Tulaczyk, J. A. Mikucki, S. A. Arcone, E. Auken, C. Schamper, and R. A. Virginia, 2015a, Subsurface imaging reveals a confined aquifer beneath an ice-sealed Antarctic lake: Geophysical Research Letters, **42**, 96–103, doi: 10.1002/2014GL062431.

Dugan, H. A., P. T. Doran, B. Wagner, F. Kenig, C. H. Fritsen, S. A. Arcone, E. Kuhn, N. E. Ostrom, J. P. Warnock, and A. E. Murray, 2015b, Stratigraphy of Lake Vida, Antarctica: Hydrologic implications of 27 m of ice: The Cryosphere, **9**, 439–450, doi: 10.5194/tc-9-439-2015.

Dugan, H. A., M. O. Obryk, and P. T. Doran, 2013, Lake ice ablation rates from permanently ice covered Antarctic lakes: Journal of Glaciology, **59**, 491–498, doi: 10.3189/2013JoG12J080.

Fritsen, C. H., and J. C. Priscu, 1998, Cyanobacterial assemblages in permanent ice covers on Antarctic lakes: Distribution, growth rate, and temperature response of photosynthesis: Journal of Phycology, **34**, 587–597, doi: 10.1046/j.1529-8817.1998.340587.x.

Fuchs, M., M. Beres, and F. S. Anselmetti, 2004, Sedimentological studies of western swiss lakes with high-resolution reflection seismic and amphibious GPR profiling: Presented at 10th International Conference on Ground Penetrating Radar, 577–580.

Jepsen, S., E. E. Adams, and J. C. Priscu, 2010, Sediment melt-migration dynamics in perennial Antarctic lake ice: Arctic, Antarctic, and Alpine Research, **42**, 57–66, doi: 10.1657/1938-4246-42.1.57.

Kanagaratnam, P., S. P. Gogineni, N. Gundestrup, and L. Larsen, 2001, High-resolution radar mapping of internal layers at the North Greenland Ice Core Project: Journal of Geophysical Research, **106**, 33799, doi: 10.1029/2001JD900191.

Kanagaratnam, P., S. P. Gogineni, V. Ramasami, and D. Braaten, 2004, A wideband radar for high-resolution mapping of near-surface internal layers in glacial ice: IEEE Transactions on Geoscience and Remote Sensing, **42**, 483–490, doi: 10.1109/TGRS.2004.823451.

Langley, K., S.-E. Hamran, K. A. Hogda, R. Storvold, O. Brandt, J. O. Hagen, and J. Kohler, 2007, Use of C-band ground penetrating radar to determine backscatter sources within glaciers: IEEE Transactions on Geoscience and Remote Sensing, **45**, 1236–1246, doi: 10.1109/TGRS.2007.892600.

Langley, K., P. Lacroix, S.-E. Hamran, and O. Brandt, 2009, Sources of backscatter at 5.3 GHz from a superimposed ice and firn area revealed by multi-frequency GPR and cores: Journal of Glaciology, **55**, 373–383, doi: 10.3189/002214309788608660.

Liu, L., Z. Li, S. Arcone, L. Fu, and Q. Huang, 2013, Radar wave scattering loss in a densely packed discrete random medium: Numerical modeling of a box-of-boulders experiment in the Mie regime: Journal of Applied Geophysics, **99**, 68–75, doi: 10.1016/j.jappgeo.2013.08.022.

McKay, C. P., G. D. Clow, D. T. Andersen, and R. A. Wharton Jr., 1994, Light transmission and reflection in perennially ice-covered Lake Hoare, Antarctica: Journal of Geophysical Research: Oceans , **99**, 20427–20444, doi: 10.1029/94JC01414.

McKay, C. P., G. D. Clow, R. A. Wharton, Jr., and S. W. Squyres, 1985, Thickness of ice on perennially frozen lakes: Nature, **313**, 561–562, doi: 10.1038/313561a0.

Murray, A. E., F. Kenig, C. H. Fritsen, C. P. Mckay, K. M. Cawley, R. Edwards, E. Kuhn, D. M. Mcknight, N. E. Ostrom, V. Peng, A. Ponce, J. C. Priscu, V. Samarkin, A. T. Townsend, P. Wagh, S. A. Young, P. T. To, and P. T. Doran, 2012, Microbial life at –13°C in the brine of an ice-sealed Antarctic lake: Proceedings of the National Academy of Sciences, **109**, 20626–20631, doi: 10.1073/pnas.1208607109.

Nedell, S. S., D. W. Andersen, S. W. Squyres, and F. G. Love, 1987, Sedimentation in ice-covered Lake Hoare, Antarctica: Sedimentology, **34**, 1093–1106, doi: 10.1111/j.1365-3091.1987.tb00594.x.

Obryk, M. K., P. T. Doran, and J. C. Priscu, 2014, The permanent ice cover of Lake Bonney, Antarctica: The influence of thickness and sediment distribution on photosynthetically available radiation and chlorophyll-a distribution in the underlying water column: Journal of Geophysical Research, **119**, 1879–1891, doi: 10.1002/2014JG002672.

Paquette, M., D. Fortier, D. R. Mueller, D. Sarrazin, and W. F. Vincent, 2015, Rapid disappearance of perennial ice on Canada's most northern lake: Geophysical Research Letters, **42**, 1433–1440, doi: http://dx.doi.org/10.1002/2014GL062960.

Parker, R., 2010, Freshwater ground penetrating radar the significance of seasonal temperature variation, *in* L. Crocco, L. Orlando, R. Persico, and M. Pieraccini, eds., Proceedings of the XIII International Conference on Ground Penetrating Radar, IEEE, 1–6.

Priscu, J. C., 2015, Ice thickness for Taylor Valley Lakes, Antarctica: Long term ecological research network, 10.6073/pasta/1e919f45c4fcc6b7229f83a08ae023ee, accessed 02 April 2015.

Priscu, J. C., C. H. Fritsen, E. E. Adams, S. J. Giovannoni, H. W. Paerl, C. P. McKay, P. T. Doran, D. A. Gordon, B. D. Lanoil, and J. L. Pinckney, 1998, Perennial Antarctic lake ice: An oasis for life in a polar desert: Science, **280**, 2095–2098, doi: 10.1126/science.280.5372.2095.

R Core Team, 2015, R: A language and environment for statistical computing: R foundation for statistical computing, http://www.R-project.org/.
Shean, D. E., and D. R. Marchant, 2010, Seismic and GPR surveys of Mullins Glacier, McMurdo Dry Valleys, Antarctica: Ice thickness, internal structure and implications for surface ridge formation: Journal of Glaciology, **56**, 48–64, doi: 10.3189/002214310791190901.
Squyres, S. W., D. W. Andersen, S. S. Nedell, and R. A. Wharton Jr., 1991, Lake Hoare, Antarctica: Sedimentation through a thick perennial ice cover: Sedimentology, **38**, 363–379, doi: 10.1111/j.1365-3091.1991.tb01265.x.
Thomas, D. N., and G. S. Dieckmann, 2010, Sea ice 2nd ed.: John Wiley & Sons.